Desalination and Water Treatment
www.deswater.com

doi: 10.1080/19443994.2015.1110719

57 (2016) 20270–20282
September

Taylor & Francis
Taylor & Francis Group

A new fluorescence index with a fluorescence excitation-emission matrix for dissolved organic matter (DOM) characterization

Jiyong Heo[a], Yeomin Yoon[b], Do-Hyung Kim[c], Heebum Lee[a], Deokjae Lee[a], Namguk Her[a,*]

[a]*Department of Civil and Environmental Engineering, Korea Army Academy at Young-Cheon, 135-1 Changhari, Kokyungmeon, Yeongcheon-si, Gyeongbuk 770-849, South Korea, emails: jiyongheo@naver.com (J. Heo), topkma41@hanmail.net (H. Lee), indramel@hanmail.net (D. Lee), Tel. +82 054 330 4755; Fax: +82 054 335 5790; email: namgukher@naver.com (N. Her)*
[b]*Department of Civil and Environmental Engineering, University of South Carolina, Columbia, SC 29208, USA, email: YOONY@cec.sc.edu*
[c]*Soil Environment Center, Korea Environmental Industry & Technology Institute, 215 Jinheungno, Eunpyeong-gu 122-706, South Korea, email: dhkim1979@naver.com*

Received 5 January 2015; Accepted 7 October 2015

ABSTRACT

A series of fluorescence approaches have been employed to characterize the composition, transformation, and biogeochemical cycles of aquatic dissolved organic matter (DOM). However, there is no consensus on the protocols for elucidating DOM fluorescence spectra from protein-like (young DOM) to humic-like (old DOM) types, which are associated with the intrinsic fluorescence properties involved in the excitation/emission and detection of DOM. The central objective of this study was to evaluate the excitation–emissions matrices (EEMs)-average area of fluorescence intensity response using DOM fluorescence spectra collected on six different DOM surrogates using high-performance size-exclusion chromatography techniques. We evaluated criteria and protocols of a new Y fluorescence index (YFI) for comparison with McKnight fluorescence index (MFI), in which 280 nm excitation coincides with independent inferences with response to emission wavelengths from 350 to 450 nm. Our results demonstrate that YFI had sufficient distinguishing power to evaluate the characteristics of organic matter, including protein- and humic-type substances under various solution conditions. In addition, the YFI has good selectivity by showing its distinct signatures at better resolution of fluorescence intensity and little variation in different solutions including wastewater effluent-derived surface water. Although MFI has the advantage of fulvic acid-oriented correction, it revealed with a narrow spectral overlap range of 0.84–2.14 for DOM characterization of Suwannee River Humic Acid (SRHA), neomycin trisulphate salt hydrate (NTH), and bovine serum albumin (BSA). This narrow range of FI for DOM surrogate was improved with YFI, implying that all NOM substances fluoresce with considerable proportional ranges of 0.30–6.41. Our results suggest that the YFI values of the DOM surrogate data-set of fluorescence EEMs are likely proportionally lower FI of pahokee peat HA and leonardite HA relative to elliott soil HA, SRHA, and SRFA, while those of NTH, Streptomycin sesquisulfate hydrate, L-tyrosine, L-tryptophan, and BSA are higher FI.

*Corresponding author.

Keywords: Fluorescence spectroscopy; Dissolved organic matter; Average area of fluorescence intensity; YFI (a new Y fluorescence index)

1. Introduction

The behavior and transport of humic substances (HSs) or natural organic matter (NOM) within aquatic systems are influenced with their heterogeneity and complex chemical structures [1–3]. They are in general naturally occurring, biogenic, heterogeneous mixture (i.e. humic acid (HA), fulvic acid (FA), lignins, carbohydrates, and proteins etc.), which are derived from the decomposition of plant and animal resides, and microbial activities [4,5]. HSs can be categorized into several groups on the basis of their solubility in alkalis and acids; for example, HA is soluble only under alkaline conditions, while FA is soluble in solutions at all pH values. This is because HA is composed of anionic macromolecules of a wide range of molecular weights with both aromatic and aliphatic components (hydrophobic) with primarily carboxylic functional groups. In contrast, FA is composed of decomposed matter from humus and peat, and has a less aromatic (hydrophilic) and more acidic character. Thus, characterization of the physicochemical properties of dissolved organic matter (DOM) should involve evaluation of its origin and fate, the reactivity and transport of inorganic and organic pollutants in the aquatic environment, and its impact on water purification and treatment processes [3].

Several fluorescence approaches based on fluorescence spectroscopy as an indicator of the general source of dissolved HA and FA in surface water, which may be correlated with the aromaticity of dissolved HSs, have been employed to elucidate DOM characteristics [6]. Furthermore, high-performance size-exclusion chromatography (HPSEC) coupled with both fluorescence and dissolved organic carbon (DOC) detectors have been used to configure pairs of fluorescent chromatography signals based on the polarity and molecular size of DOM [7–11]. The HPSEC-fluorescence spectroscopy system facilitated classification of protein-, polysaccharide-, fulvic-, and humic-like groups from microbially and terrestrially derived organic material in water ecosystems. McKnight et al. [6] proposed the use of the McKnight fluorescence index (MFI), in which the two-dimensional fluorescence intensity was scanned at wavelengths of 450–500 nm and an excitation wavelength of 370 nm. The MFI categorized FA into microbially and terrestrially derived types containing distinctive fluorophores based on MFI values of ~1.4 and ~1.9, respectively.

Use of fluorophore distribution to characterize DOM has focused on three-dimensional excitation–emissions matrices (EEMs), which facilitated prediction of DOM behavior in both natural water and engineered treatment systems [12–14]. Several studies have shown that use of EEMs enables detection of various DOM fractions (i.e. proteins and HSs) because DOM properties relate to chromophoric (light absorbing) and fluorophoric (light emitting) moieties by their intrinsic fluorescent characteristics [15–18]. To address the fluorescence spectra of EEMs, a series of methods involving correlations of DOM specificities and fluorescent groups have been suggested [19,20]. The EEM-fluorescence regional integration (FRI) method was developed to distinguish EEMs by quantitatively integrating all intensities within designated regions [1,18,21,22]. The FRI method is based on the various DOM having different fluorophore groups. Chen et al. [1] operationally classified excitation and emission wavelength boundaries into five EEM regions and integrated underneath EEM intensities to calculate the cumulative fluorescence spectra; for instance, the cumulative intensities of shorter excitation wavelengths (<250 nm) and emission wavelengths (<350 nm) were classified as simple aromatic proteins. Regarding the EEMs-multi-way data analysis of parallel factor analysis (PARAFAC), a statistical modeling approach to characterizing EEMs of DOM, allows minimization of the different independent groups of data-sets of fluorophores [15,23–25]. Thus, it allows comparisons of the shift in DOM fluorophore wells as a function of redox state, as well as identification of the interactions of trace metals and fluorescence quenching titrations in DOM [26,27], and tracking of changes in DOM characteristics during water treatment processes [28].

With these series of fluorescence approach considerations, quantitative variation in the fluorescence index (FI) depends on the peak fluorescence intensity, which could be variable due to constrained optimization, the proportions of precursor organic materials, and inner-filter light scattering caused by metal complexation. Compared to EEMs-FI, EEMs-FRI may be useful for refining DOM fractions for field studies, which could also be used with other water quality data to infer DOM characteristics relevant to their composition, transformation, and biogeochemical cycles in streams and rivers.

This study applied quantitative HPSEC-EEMs-FRI techniques to analysis of DOM surrogates, such as the IHSS Suwannee River HA and FA. The analysis based on DOM surrogates of known origin facilitated comparison of the MFI and spectral techniques of average fluorescence intensity. The average fluorescence intensity techniques were contrasted with MFI in terms of classifying DOM surrogates, in which a new average fluorescence intensity method (YFI, a new Y Fluorescence Index) was applied to quantitative application through the average intensity of specific emission and excitation wavelengths with HPSEC-EEMs. This study also compared the variations in MFI and YFI in aqueous solutions of various chemistries and with different surface water properties.

2. Materials and methods

2.1. Reagents and selection of DOM surrogates

Analytical grade chemicals were obtained from Sigma–Aldrich, USA. HCl and NaOH (0.1 M) were to adjust pH, and aliquots of 1 mM $NaHCO_3$ and 20 mM NaCl for the background electrolyte of conductivities. Several DOM surrogates (Sigma–Aldrich, USA) were selected to represent the main organic matter groups found within water and wastewater, including amino sugars and proteins. Proteins and amino acids are important components of DOM and are commonly used materials in evaluations of DOM characteristics; these were represented by allochthonous DOM surrogates of a principally hydrophilic nature. Suwannee River standard FA (cat. no. 1S101F), HA (cat. no. 2S101H), pahokee peat HA (cat. no. 1R101 N), leonardite HA (cat. no. 1R101 N), and elliott soil HA (cat. no. 1R101 N) were purchased from the International Humic Substance Society (IHSS, USA). Streptomycin sesquisulfate hydrate (SSH), neomycin trisulphate salt hydrate (NTH), L-tyrosine (LTRS), L-tryptophan (LTTP), and bovine serum albumin (BSA) were purchased from Sigma–Aldrich, USA. Solid samples were dissolved in pure water and filtered through a 0.45 μm Millipore-syringe filter to remove insoluble particulate materials, and were used without further purification. Selected characteristics of the bulk NOM surrogates used in this study and their origins, molecular formulae, molecular weights, atomic ratios, and aromatic contents are provided in Table 1.

2.2. HPSEC and fluorescence EEMs

The preserved samples were divided into two aliquots; one was used for determination of MW and DOC concentrations by HPSEC; the other was subjected to fluorescence EEM analysis. HPSEC was performed using a binary pump SL (flow range: 0.001–5 mL/min), a micro-vacuum degasser, diode array detector SL (spectral analysis: 8 signals, 80 Hz data rate), and equipped with a silica gel column (TOSOH TSKgel G2000SWXL G3000SWXL; i.d. 7.8 mm, length 30 cm). Reverse-phase separations were conducted with a 100 μL sample loop, of length 25 cm and inner diameter 2 cm. HPSEC analyses were performed using an isocratic elution mode with a mobile phase mixture of phosphate buffer. This was operated for 20 min at a constant flow rate of 1 mL/min; a sample injection volume of 2 mL was used. Generally, among NOM surrogates, hydrophilic components are regarded as having shorter retention times, whereas those with hydrophobic characteristics have longer retention times. A DOC (Modified Sievers Total Organic Carbon Analyzer 800 Turbo) detector with an autosampler was used for optimization tracking of separated NOM components, which was the oxidation method with acid addition and external sparging to remove inorganic carbon. A polyethylene glycol (PEG) standard of MW 200–10,000 Da was used as the HPSEC calibrant. Calibration was conducted for all analyses, and calibration curves yielded stable values under all experimental conditions tested. The resultant calibration curve was used to estimate the MW (Da) of samples as a function of retention time. NOM samples were subjected to 3-D EEM fluorescence spectra measurement.

The obtained fluorescence spectra are representative of the molecular weight distribution of the fluorophores within DOM samples. The 3-D EEM fluorescence spectra were determined using a Perkin Elmer LS50B fluorescence spectrophotometer (Perkin Elmer, New Jersey, USA) with both excitation and emission monochromators; a xenon lamp at a PMT voltage of 700 V was used as the excitation source. The fluorescence emission spectra were determined using a range of excitation wavelengths to provide a simultaneously subsequent scanning of EEM spectra (emission wavelength from 300 to 550 nm in 5 nm increments by varying the excitation wavelength from 250 to 500 nm at 5 nm intervals, respectively). According to the EEM spectra, the analytical conditions were set as described in Table 2. For scanning, the fluorescence intensities were monitored with a band-pass width of 5 nm for excitation and 10 nm for emission at a scan speed of 2,400 nm min^{-1}. The blank spectra identification was adjusted by Milli-Q water as blank to minimize water Raman scattering. Various ionic strength and pH values were used to evaluate the influence of water chemistry on EEM studies of DOM

Table 1
The characteristics of NOM surrogates

Category	Organic type	Molecular formula	MW (g/mol)	Origin in water	Carbon content (%)	Atomic ratio			Aromatic content (%)	Amino Acid Compositions (μmol/g)	Carbohydrate Compositions (μmol/g)	Refs.
						H/C	O/C	C/N				
Fulvic-like	SRFA (Suwannee River Fulvic Acid)	–	1,240	Peat deposits	52.4	0.98	0.60	84.96	22	24	43	[38]
Humic-like	SRHA (Suwannee River Humic Acid)	–	2,090	Peat deposits	52.6	1.00	0.61	51.51	31	89	97	
	PPHA (Pahokee Peat Humic Acid)	–	8,500	Organic deposits of freshwater marshes	56.4	0.81	0.50	17.82	–	373	100	
	LHA (Leonardite Humic Acid)	–	11,661	Brown–black, oxidized form of lignite coal	63.8	0.69	0.37	60.52	58	11	3	
	ESHA (Elliott Soil Humic Acid)	–	19,000	Peat and decomposing vegetation	58.1	0.75	0.44	16.38	50	777	206	
Aminosugar-like	SSH (Streptomycin Sesquisulfate Hydrate)	$C_{21}H_{39}N_7O_{12}$	581.6	Derived from the actinobacterium *Streptomyces griseus*	43.4	1.86	0.57	3.00	–	–	–	[39]
	NTH (Neomycin Trisulfate Salt Hydrate)	$C_{23}H_{46}N_6O_{13}$	614.6	Aminoglycoside antibiotic	45.0	2.00	0.57	3.83	–	–	–	
Protein-like	LTRS (L-tyrosine)	$C_9H_{11}NO_3$	181.2	1 of the 22 standard amino acids	59.7	1.22	0.33	9.00	–	–	–	[40]
	LTTP (L-tryptophan)	$C_{11}H_{12}N_2O_2$	204.2	1 of the 22 standard amino acids	64.7	1.09	0.18	5.50	–	–	–	
	BSA (Bovine Serum Albumin)	–	66,500	Derived from cows	50–55	1.57	0.31	3.76	–	–	–	[41]

Table 2
Analytical conditions used for the Y fluorescence index (YFI)

pH	Temp. (°C)	Ionic strength (mS/cm)	Concentration (mgC/L)	
6.8	10, 20, 30	0.05, 0.7, 1.4	1, 3, 5	
Excitation wavelengths (nm)	Range of emission wavelengths (nm)			
280	300–350	351–400	401–450	451–500

surrogates. Approximately 1.4 mL of the sample was introduced to the target and placed in a Spectrosul Far UV quartz triangular fluorescence cell. Fluorescence measurements were conducted at 20°C using Thermo-chiller.

2.3. Fluorescence index calculations and data processing

The desirable formulation can lead to determination when attempting to apply the interpolation method obtained from the average area of fluorescence intensities against emission ranges for each excitation by normalizing the cumulative excitation–emission area to relative regional areas. In this study, the 3D-EEM spectra were corrected for fluorescence regional index analysis, in which the fluorescence intensities were presented as YFI values together with the average cumulative area of each excitation–emission range. This range was selected to better reveal the configuration and to minimize the effects of Rayleigh and Raman scattering that FRI yielded better DOM characteristics and heterogeneity compared to the FI method. It was also confirmed using dilution series of DOM standards, such as the IHSS Suwanee River FA, which suggested that the average fluorescence intensities in this range were highly linear and reliable. Additionally, this range was considered and duly weighed with the literature survey. The interpolation was used for fluorescence EEM data processing and YFI (a newly defined Y Fluorescence Index, Y stands for Yeomin) was calculated using the following equation:

$$\text{YFI} = \text{FEI range of } 350{:}400/\text{FEI range of } 400{:}450 \times (\text{a } \lambda_{Ex} \text{ of } 280\,\text{nm}) \quad (1)$$

where the YFI is calculated as the ratio of the corrected average fluorescence intensities in the range of 350:400 over 400:500 (a λ_{Ex} of 280 nm). FEI range of 350:400 refers to the average fluorescence intensities of the entire range between the λ_{Em} range of 350–400 nm and a λ_{Ex} of 280 nm for the average fluorescence intensity method.

3. Results and discussion

3.1. DOM surrogate classification

The DOM surrogate was fractionated into four classes based on the van Krevelen 3D-diagrams according to the hydrogen to carbon atomic ratio (H/C), the oxygen to carbon atomic ratio (O/C), and the carbon to nitrogen atomic ratio (C/N) (Fig. 1); this is because it mainly contains the C of biogeochemical cycle and experiences the structural changes by the degree of maturity of DOMs based on the different natural circumstances. Van Krevelen 3D-diagrams have been used to graphically present elemental compositions (i.e. hydrophobic, hydrophilic, and/or amphiphilic fractions), in which the H/C and O/C ratios of DOM surrogates correlated with the degree of decomposition [29–32]. Such diagrams indicate the humification process in terms of the degree of maturity and intensity of degradation processes; e.g. the increased ring condensation (increase in the H/C ratio), decarboxylation (reduction in the O/C ratio), and demethylation that occur during the decay of peat-forming plants, and peat humus maturation into coal.

Atmospheric functionalization of the DOM surrogate, including aging effects (i.e. oxidation,

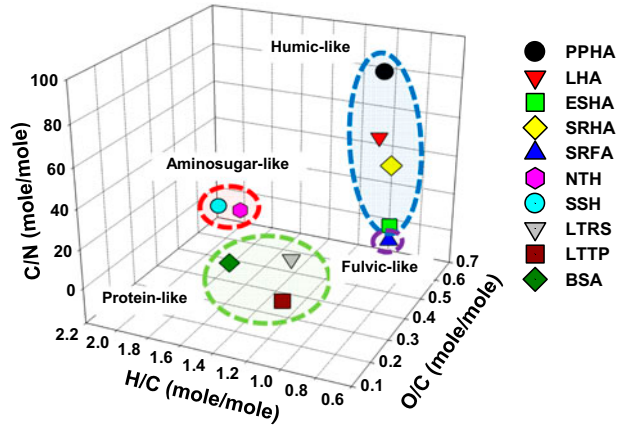

Fig. 1. Van Krevelen 3D diagrams showing the H/C, O/C, and C/N ratios of NOM surrogates from the assigned formulae (C, H, O).

volatilization, and condensation), is generally defined by changes not only in the O/C ratio but also the H/C ratio. The combination changes are especially evident of aging effects if the H/C and O/C atomic ratios of protein- and aminosugar-like substances (lower O/C and higher H/C in Fig. 1) are compared to those of fulvic- and humic-like substances of a high degree of decomposition (higher O/C and lower H/C in Fig. 1). Only non-oxidation reactions, such as ambiguously aminosugar-like (higher O/C ratio), can be used to describe the aging effect, in which the hydration process shows no changes through the O/C ratio by transforming alcohol to carbonyl functionalization. The empirical aging factor takes into account the fact that protein- and aminosugar-like substances have a lower C/N ratio in living organic matter than humic organic matter. This difference in C:N ratios is indicative of the different characteristics of DOM surrogates. Protein- and aminosugar-like substances are indicative of the beginning of transformation of organic matter. They are formed by a process in which the more labile structures (protein, carbohydrates, amino acids, etc.) are destroyed and utilized through nitrogen mineralization, but more stable aromatic and polyaromatic organic compounds are formed in the atmosphere where the most oxidized humic species are located at the lower right, as shown in Fig. 1. The van Krevelen 3D diagram demonstrated that the humification degrees of DOM surrogates are consistent with their H/C, O/C, and C/N atomic ratios; hence, such diagrams can be used to characterize DOM transformation processes.

3.2. Selection of a method of generating a reproducible average fluorescence intensity

The EEM spectra of DOM surrogate provide the typically distinct locations of fluorescence peaks in their excitation and emission maxima, which can be used to calculate a fluorescence index. A metric of fluorescence peaks, EEMs are attributable mainly to the presence of common fluorophores in DOM surrogates, which are classified into tryptophan-like (proteins and peptides), tyrosine-like (aminosugar), fulvic-like, and autochthonous/allochthonous humic-like materials. These peaks occur in fluorescence spectra, which was indicated with the range of common type of DOM surrogate included protein-like peaks (λ_{Ex} 270–285 nm, λ_{Em} 310–360 nm), fulvic-like peaks (λ_{Ex} 320–350 nm, λ_{Em} 400–450 nm), and humic-like peaks (λ_{Ex} 310–450 nm, λ_{Em} 380–520 nm). The fluorescence intensity of BSA (λ_{Ex} 280 nm, λ_{Em} 300–500 nm; Fig. 2) exhibited characteristics suggesting that it could be used to derive a fluorescence-derived index. The average regional index of fluorescence spectra were applied because of its benefits to be able to handle over all intensities through the wide reference of DOM surrogate compared to the typical range of excitation or emission wavelength.

Based on the fluorescence spectrum of BSA, the typical diagonal boundaries were drawn within first- and second-order Rayleigh scattering positions. The boundary separated into four ranges (designated A to D) as shown in Fig. 2. The area locations of B and C, including water level radiation intensity, were discarded to minimize the variations for photochemical process for DOM surrogate. In this study, YFI was determined using excitation at 280 nm with the average intensity of the fluorescence ratio of B over C, which was expected to remain constant among the various water chemistry environments. Since protein-like fluorescence was rarely detected in any fluorescence spectrum indices, most are characterized using the humic-like fluorescence area. Thus, in this study, the simplification fluorescence average index method of the DOM surrogate including protein (young DOM) to HSs (old DOM) was characterized using the median intensity value of the florescence ratio. Fluorescence quenching effects due to solution chemistry and overlapping effects of fluorophore yields were considered during selection of fluorescence intensities as quantification of these effects was precluded by the unknown optical properties of discrete isomers within the DOM surrogate used in this study.

A blank experiment was performed to identify the optimum wavelength for each wavelength combination within the fluorescence matrix, and no further correction of YFI was performed. Spectral subtraction

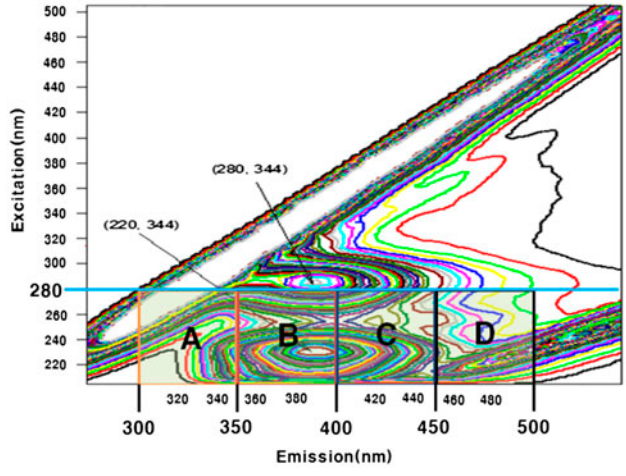

Fig. 2. Fluorescence photographs of BSA at excitation wavelengths of 260–300 nm.

was performed to remove blank spectra mainly caused by Raman scattering. Fig. 3 suggests that the variations in the average area of fluorescence ratio in specific classes of the excitation wavelength of Suwannee River Humic Acid (SRHA), which was different in those conditions (conductivity, 0.05–5.1 mS/cm; temperature, 10 and 30˚C). According to the average fluorescence intensity, protein-like types were well reposed at an excitation of 280 nm and emission wavelengths of 300–400 nm, and the YFI values (the ratio of B over C at various solution chemistries) were similar under each condition. Generally, the intensity of YFI decreased with increasing solution temperature and was more highly variable at excitation wavelengths of 260, 270, 290, and 300 nm compared to 280 nm, especially in low IS (Fig. 3(a)). At high IS values, YFI intensity was maximum at 280 nm and decreased with increasing solution temperature as well as decreasing IS (Fig. 3(b)). This was likely due to the following reasons: (i) DOM surrogate fluorophore formation and water level radiation intensity became important in the B range (in Fig. 2) near the first-order Rayleigh scattering position, which gives increasing intensities with decreasing temperature, (ii) the intensity of samples was little quenched with the relative intensity contribution of DOM fluorophores at 280 nm compared to other excitation wavelengths (260–270, and 290–300 nm), which was expected to persist irrespective of IS effects and temperature variations. The minimum variation in YFI at excitation at 280 nm with BSA was reasonable because protein-like substances exhibited high intensities in this area. Although DOM possesses humic characteristics, it exhibited low variation as the two fluorophores overlapped in this range, related to FI and humification index (HIX) [33,34] values. The varying IS and solution temperature appeared to have little effects on the YFI (B over C at 280 nm) spectral characteristics of DOM surrogates.

3.3. Average fluorescence intensity analysis under various conditions

Application of numerous fluorescence indices; e.g. biological/autochthonous index (BIX) [35], and HIX [33,34], has facilitated evaluation of a large number of structural and functional groups and their compositions in DOM surrogates. DOM surrogates contain aromatic structures (humic-like types) with various functional groups and heterogeneous components containing unsaturated fatty acid chains (protein-like types), which influence the fluorescence characteristics. It was assumed that EEM fluorescence spectroscopy facilitates accurate determination of the general patterns of DOM surrogates and should be unaffected by various conditions in terms of its ability to detect anthropogenic functional groups within DOM substances. However, EEM fluorescence spectroscopy has shown high sensitivity due to its substantial character and susceptible selectivity. In addition, the presence of functional groups within DOM surrogates affects the results of EEM spectroscopy because functional groups can be related to the solution chemistry conditions, such as pH, ionic strength, temperature, sample concentration, etc. [36].

As shown in Fig. 4, 280 nm excitation coincides with the intensities of DOM surrogates relating to the response to emission wavelengths of 350–450 nm. Using this fluorescence range, the YFI facilitated characterization of protein- and humic-type substances in organic matter of various origins. The selectivity of YFI was demonstrated by its determination of fluorescence intensity values of 0.45, 2.02, and 6.0 for SRHA, NTH, and BSA, respectively. It was observed to be distinct signatures of having a better resolution of intensity and little variation in various solution conditions as shown in Fig. 4 (arrows indicates variations). The utility of YFI for characterization of SRHA, NTH,

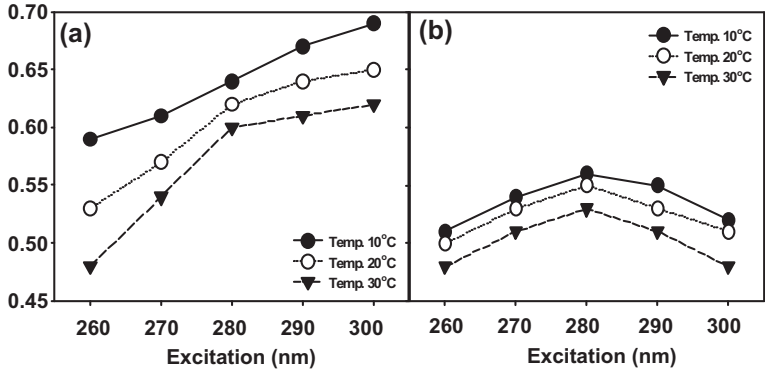

Fig. 3. Selection of the optimum excitation wavelength for YFI. (a) pH 6.8, Conductivity 0.05 mS/cm, Temp. 10–30˚C, Conc. SRHA 5 ppm and (b) pH 6.8, Conductivity 5.1 mS/cm, Temp. 10–30˚C, Conc. SRHA 5 ppm.

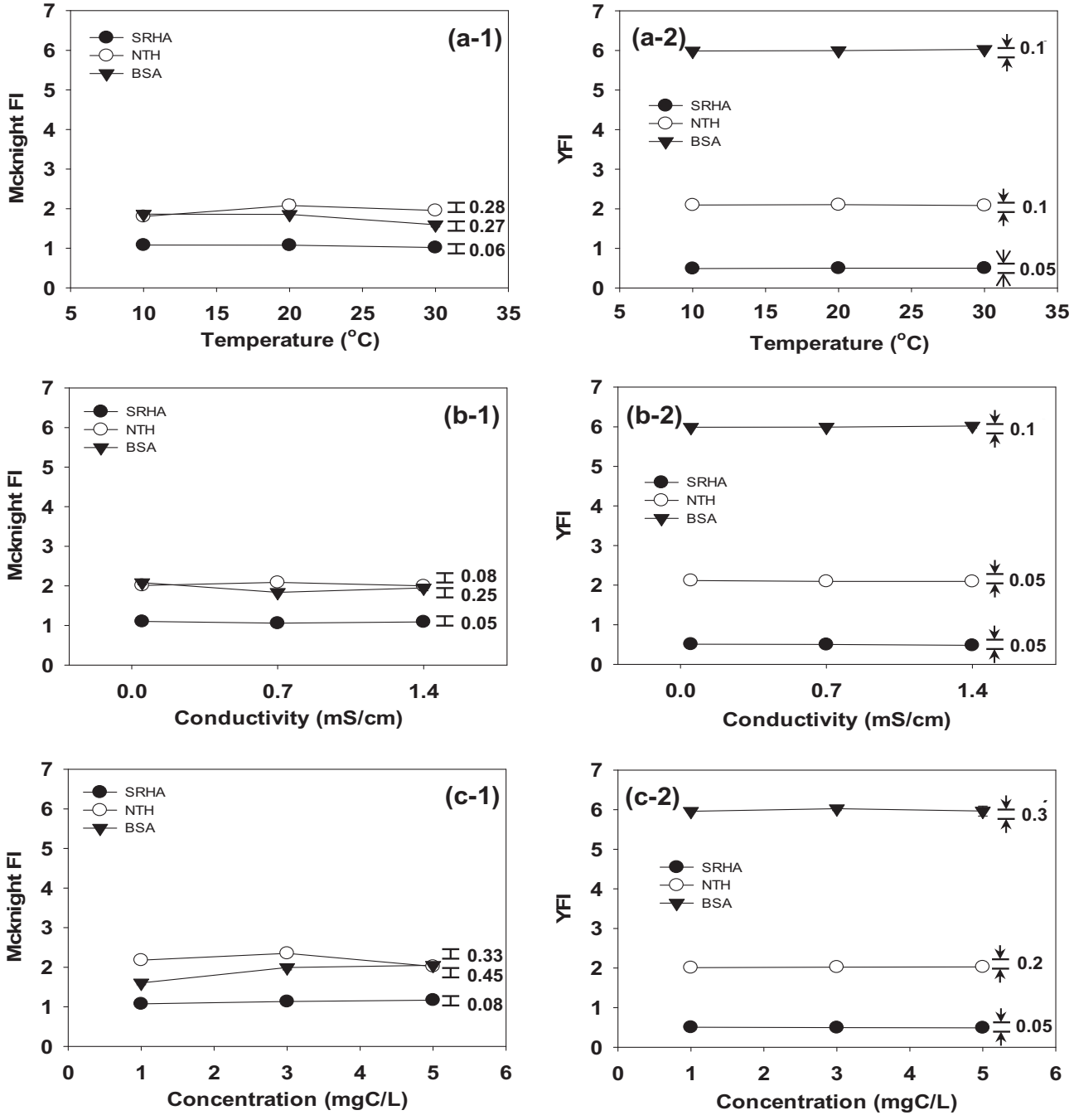

Fig. 4. Comparison of McKnight FI and YFI under various conditions: (a) pH 6.8, Conductivity 0.7 mS/cm, Temp. 10–30℃, Conc. 3 ppm, (b) pH 6.8, Conductivity 0.05–1.4 mS/cm, Temp. 20℃, Conc. 3 ppm, and (c) pH 6.8, Conductivity 0.7 mS/cm, Temp. 20℃, Conc. 1–5 ppm.

and BSA is consistent with the fact that the fluorescence values of all DOM substances and have a clear gap of proportional ranges from 0.49 to 6.03 (Fig. 4(a), (b), and (c-2)), while the MFI has a very narrow gap and fluctuation of proportional ranges from 1.01 to 2.08 (Fig. 4(a), (b), and (c-1)).

In particular, the NTH and BSA fractions showed a similar MFI of ~2.1 (Fig. 4(a), (b), and (c-1)), which has a small discrepancy of fluorescence index due to the barely discernible values of the NTH and BSA fractions. Such minor discrepancies in the MFI values were attributable primarily to the arbitrary definition

of the fluorescence index (the E_{450}/E_{500} ratio intensity), so that the weak MFI intensities occurred at the peak fluorophore positions of fluorescence EEMs in NTH and BSA. The NTH and BSA were to be formed a comparatively shorter emission wavelength range and also their intensity in longer wavelength were appeared to be no discernible vibration trends. Regarding reproducibility, YFI showed indistinguishable differences under various solution conditions, especially temperature, conductivity, and concentration. In contrast, the MFI showed significant variations under the same conditions (Fig. 4(a), (b), and (c-1)). The YFI variations for SRHA, NTH, and BSA were less than 0.05, 0.2, and 0.3, respectively; the equivalent values for the MFI were 0.08, 0.33, and 0.45, for a temperature of 10–30˚C, conductivity of 0.05–5.1 mS/cm, and DOC concentration from 1 to 5 mgC/L, respectively. Thus, YFI can be used to identify the fluorescent compounds present in complex NOM mixtures from various origins.

Effluent organic matter (EfOM) derived from surface water is considered to have a heterogeneous composition comprising complex aquatic humic and non-humic substances (i.e. biopolymers). The non-humic substances are represented by extracellular polymeric substances (EPS) comprising proteins, polysaccharides, nucleic acids, lipids, HAs, etc. The fluorescence intensity of complex aquatic DOM (and their multiple oxidation states) is affected by the mixture of HSs attached with the substrates of non-humic substances. Thus, FI can be used to investigate the DOM present in wastewater effluent-derived surface water, and the fluorescence characteristics under various solution conditions (temp., conduc., and conc. of DOM) are shown in Fig. 5. Application of the MFI to the analysis of surface waters from Nakdong, Hwang, and the Kumho River with various solution conditions (same with DOM surrogates), in which the DOM was extracted from the core samples using NaOH, resulted in detection of marked fluctuations (gradual increases

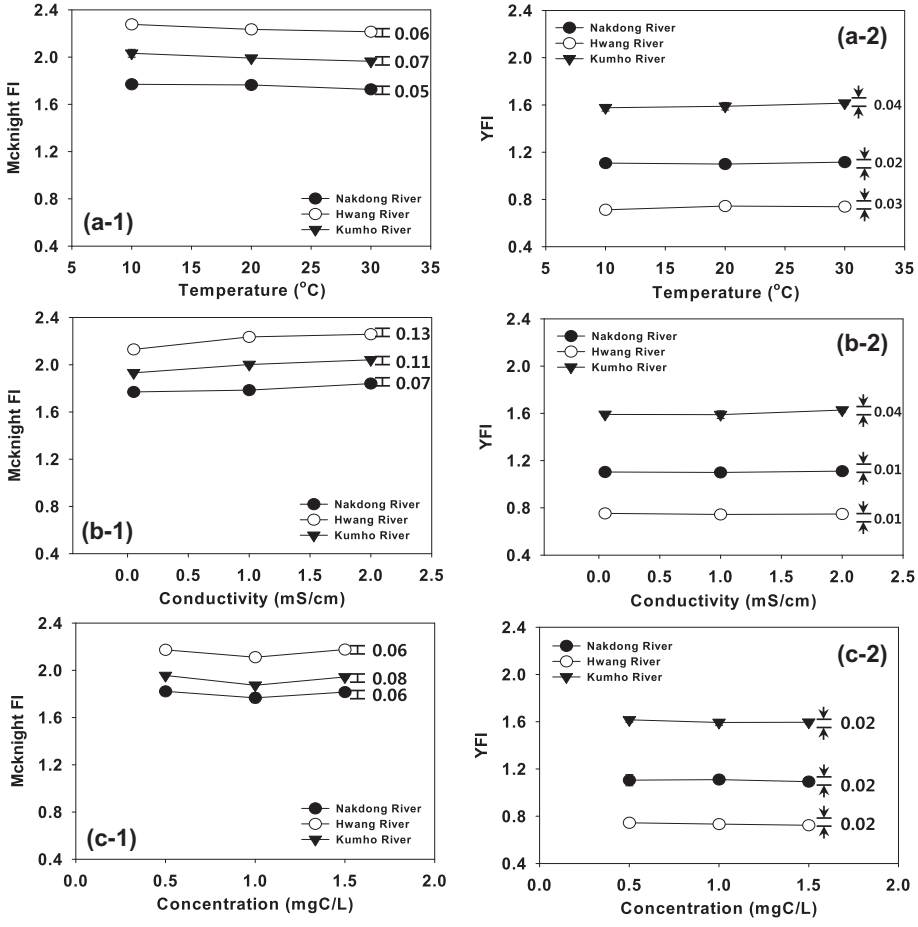

Fig. 5. Comparison of McKnight FI and YFI for NOMs in surface water: (a) pH 6.8, Conductivity 1 mS/cm, Temp. 10–30˚C, conc. 1 ppm, (b) pH 6.8, Conductivity 0.05–2 mS/cm, Temp. 20˚C, conc. 1 ppm, and (c) pH 6.8, conductivity 1 mS/cm, Temp. 20˚C, conc. 0.5–1.5 ppm.

or decreases, Fig. 5(a), (b), and (c-1)). The YFI for the Nakdong, Hwang, and the Kimho River were 0.71, 1.1, and 1.61, respectively, regardless of solution conditions. YFI toward Nakdong, Hwang, and the Kumho River are consistent with the fact that the fluorescence intensities of DOM substances have the clear gap and small discrepancy of FI of proportional ranges from 0.71 to 1.61 (variation was less than 0.04), while the MFI has the very narrow proportional gap and big discrepancy ranged from 1.72 to 2.23 (variation was less than 0.13). The peak locations in YFI were independent of the DOM concentration, but the peak intensity in the MFI was strongly dependent on the DOM concentration. This might be attributable to the inner filtering configuration effect (different Peak A to Peak B intensity ratios for both surface water spectra) to drive the FI. Fig. 5(b-2) shows YFI values and EEM fluorescence spectral characteristics of surface waters with various ionic strengths. The peak locations, intensities, and ratios in the EEM spectra of the surface water samples were not affected markedly by ionic strength. These results are in good agreement with those of Mobed et al. [37], who suggested that ionic strength had no considerable effect on the EEM spectra of aquatic or soil-derived HSs.

The comparison of MFI and YFI, surface water characterized by a lower FI intensity was correlated with terrestrially derived DOC sources, because high FI values are thought to correlate with both the aromaticity of autochthonous organic matter and HSs attached with substrates of non-humic substances. In this study, the MFI and YFI exhibited different tendencies. The MFI values were in the order Hwang > Kumho > Nakdong Rivers, compared to Kumho > Nakdong > Hwang Rivers for YFI values. These YFI results were different from the MFI values, in which the DOM fluorescence intensities decreased with increasing levels of terrestrially derived DOC. This might be attributed to the changes in fluorescence characteristics with the different arbitrary range of the organic macromolecular fluorophores, as well as the changes of their configurations of designated main intensity calculations.

3.4. Average fluorescence intensity analysis of NOM surrogates

EEM intensity is represented with contour lines. The average regional intensities of excitation–emission wavelength boundaries selected to characterize EEMs were operationally utilized for the same NOM surrogate samples. Using YFI, the distinct peak ratios at different emission wavelength boundaries suggest that the fluorophores present in samples differed according

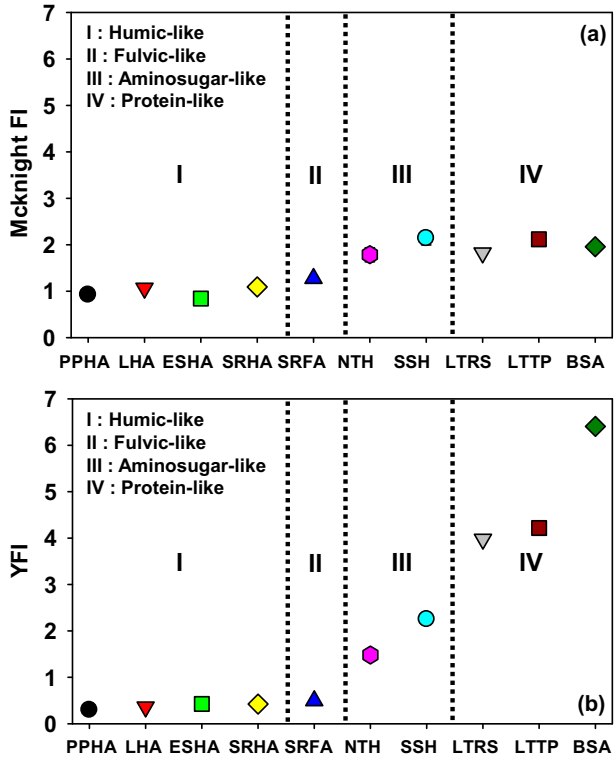

Fig. 6. (a) McKnight FI and (b) YFI values of NOM surrogates (pH 6.8, Con. 5.1 mS/cm, Temp. 20℃, Conc. 5 ppm).

to their origin. The arrangement of NOM surrogates was based on the FI, as shown in Fig. 6 (the MFI and YFI values for NOM surrogates have different boundaries from ranges I–IV).

When applying MFI and YFI values, the YFI shows the specific and clear response from sample spectra through all selected NOM surrogates, in which they were deployed in sequence by fluorescence index, and differences in NOM surrogates EEMs collected on different boundaries. A higher density of EEM fluorescence-absorbing functional groups corresponds to the lowest for humic and fulvic-like (0.36 for LHA, fluorophores in a lowest range of in the YFI response emission wavelengths), medium for aminosugar-like (2.25 for SSH, fluorophores in an intermediate range of in the YFI response emission wavelengths), and highest for protein-like (6.41 for BSA, fluorophores located in a highest range of in the YFI response emission wavelengths) types. For the intrinsic YFI parameters of NOM surrogates, these indices increased as NOM origin was increased from 0.30 to 6.41. On the other hand, for the MFI, these ratios slightly increased as from humic- to aminosugar-like was changed from 0.84 to 2.14, and only vaguely changed thereafter in the protein-like ranges. Such differences confirm that

the fluorescence characteristics of the McKnight FI and YFI differed. The YFI thus facilitates discrimination of protein-like substances from other NOM components. However, for the MFI values of aminosugar and protein-like, this trend was found to be not robust between them. Especially, the MFI of protein-like substances showed little difference compared to YFI, for the following reasons: (i) with the increase in the proportions of aminosugar- and protein-like materials, this peak was clearly seen at shorter emission range due to a higher intensity peak corresponding to the chromophores properties of organic matter connected to amides from protein-like substances. A higher density of functional (e.g. amino acids, peptides, and proteins) groups corresponds to a higher intensity at shorter wavelength (~210 nm), resulting in producing a higher YFI. Thus, the ratio of the absorbance at 280 nm to that of the YFI emission wavelength is greater for proteins and amino acids than for HSs. (ii) The YFI value of humic-like substances, (<0.5) implies the lowest proportions of aromatic rings in the YFI response ranges, in which the aromatic groups of humic materials mainly associated with weaker intensities for SRHA than for protein-like materials.

4. Conclusions

While various spectroscopic techniques, including HPSEC-EEMs-average fluorescence intensity, are employed for investigations of DOM characteristics, they provide qualitative as opposed to quantitative information. In this study, we evaluated average fluorescence intensities at the same excitation wavelength (280 nm) of the PPHA, LHA, ESHA, SRHA, SRFA, NTH, SSH, LTRS, LTTP, and BSA surrogates in their entire emission ranges (350–450 nm) to identify the indices of humic and proteinaceous substances. Thus, the YFI is defined as the ratio of the corrected average fluorescence intensities at 350:400 to that at 400:450 [nm] with a λ_{Ex} of 280 nm. Regarding humic-like substances (old NOM origin), the EEM showed peak maxima at a longer emission wavelength, which resulted in lower YFI values. Similar peaks were found at a longer emission wavelength for PPHA, LHA, ESHA, and PPHA. This may be attributable to the large amounts of functional groups and aromatic rings in humic-like materials being excited by longer emission wavelengths. In contrast, protein-like substances exhibited higher YFI values compared to humic-like substances due to the higher intensity at shorter wavelength (~210 nm) derived from the interaction between the N–H bonding and C–N stretching of the C–N–H group.

The YFI analysis thus facilitated discrimination of protein-like substances from other NOM components. SRHA showed a low YFI value with the old organic matter fractions, similar to PPHA and LHA. It has been strongly associated with terrestrial organic matter participation to, and anticipated to contribute proportionately lower YFI values. With the application of YFI analysis, it showed trends to the lowest YFI values for humic and fulvic-like (PPHA, LHA, ESHA, SRHA, and SRFA), medium for aminosugar-like (NTH and SSH), and highest for protein-like (LTRS, LTTP, and BSA) substances.

Acknowledgments

This research was supported by the Korean Ministry of Environment, GAIA Project, 2015000540003.

References

[1] W. Chen, P. Westerhoff, J.A. Leenheer, K. Booksh, Fluorescence excitation−emission matrix regional integration to quantify spectra for dissolved organic matter, Environ. Sci. Technol. 37 (2003) 5701–5710.
[2] M. Filella, Understanding what we are measuring: Standards and quantification of natural organic matter, Water Res. 50 (2014) 287–293.
[3] A. Matilainen, E.T. Gjessing, T. Lahtinen, L. Hed, A. Bhatnagar, M. Sillanpää, An overview of the methods used in the characterisation of natural organic matter (NOM) in relation to drinking water treatment, Chemosphere 83 (2011) 1431–1442.
[4] N. Her, G. Amy, D. McKnight, J. Sohn, Y. Yoon, Characterization of DOM as a function of MW by fluorescence EEM and HPLC-SEC using UVA, DOC, and fluorescence detection, Water Res. 37 (2003) 4295–4303.
[5] J. Swietlik, E. Sikorska, Characterization of natural organic matter fractions by high pressure size-exclusion chromatography, specific UV absorbance and total luminescence spectroscopy, Pol. J. Environ. Stud. 15 (2006) 145.
[6] D.M. McKnight, E.W. Boyer, P.K. Westerhoff, P.T. Doran, T. Kulbe, D.T. Andersen, Spectrofluorometric characterization of dissolved organic matter for indication of precursor organic material and aromaticity, Limnol. Oceanogr. 46 (2001) 38–48.
[7] F.H. Frimmel, Characterization of natural organic matter as major constituents in aquatic systems, J. Contam. Hydrol. 35 (1998) 201–216.
[8] S. Velten, D.R.U. Knappe, J. Traber, H.-P. Kaiser, U. von Gunten, M. Boller, S. Meylan, Characterization of natural organic matter adsorption in granular activated carbon adsorbers, Water Res. 45 (2011) 3951–3959.
[9] S. Valencia, J. Marín, J. Velásquez, G. Restrepo, F.H. Frimmel, Study of pH effects on the evolution of properties of brown-water natural organic matter as revealed by size-exclusion chromatography during photocatalytic degradation, Water Res. 46 (2012) 1198–1206.

[10] S.H. Valencia, J.M. Marín, G.M. Restrepo, Evolution of natural organic matter by size exclusion chromatography during photocatalytic degradation by solvothermal-synthesized titanium dioxide, J. Hazard. Mater. 213–214 (2012) 318–324.
[11] N. Her, G. Amy, H.-R. Park, M. Song, Characterizing algogenic organic matter (AOM) and evaluating associated NF membrane fouling, Water Res. 38 (2004) 1427–1438.
[12] K.K. Mueller, C. Fortin, P.G. Campbell, Spatial variation in the optical properties of dissolved organic matter (DOM) in lakes on the Canadian precambrian shield and links to watershed characteristics, Aquat. Geochem. 18 (2012) 21–44.
[13] K. Chon, J. Cho, H.K. Shon, Advanced characterization of algogenic organic matter, bacterial organic matter, humic acids and fulvic acids, Water Sci. Technol. 67 (2013) 2228–2235.
[14] J. Chen, E.J. LeBoeuf, S. Dai, B. Gu, Fluorescence spectroscopic studies of natural organic matter fractions, Chemosphere 50 (2003) 639–647.
[15] R.M. Cory, D.M. McKnight, Fluorescence spectroscopy reveals ubiquitous presence of oxidized and reduced quinones in dissolved organic matter, Environ. Sci. Technol. 39 (2005) 8142–8149.
[16] R.M. Cory, M.P. Miller, D.M. McKnight, J.J. Guerard, P.L. Miller, Effect of instrument-specific response on the analysis of fulvic acid fluorescence spectra, Limnol. Oceanogr. Methods 8 (2010) 67–78.
[17] M.S. Johnson, E.G. Couto, M. Abdo, J. Lehmann, Fluorescence index as an indicator of dissolved organic carbon quality in hydrologic flowpaths of forested tropical watersheds, Biogeochemistry 105 (2011) 149–157.
[18] J.A. Korak, A.D. Dotson, R.S. Summers, F.L. Rosario-Ortiz, Critical analysis of commonly used fluorescence metrics to characterize dissolved organic matter, Water Res. 49 (2014) 327–338.
[19] W.-T. Li, Z.-X. Xu, A.-M. Li, W. Wu, Q. Zhou, J.-N. Wang, HPLC/HPSEC-FLD with multi-excitation/emission scan for EEM interpretation and dissolved organic matter analysis, Water Res. 47 (2013) 1246–1256.
[20] J.E. Birdwell, A.S. Engel, Characterization of dissolved organic matter in cave and spring waters using UV–vis absorbance and fluorescence spectroscopy, Org. Geochem. 41 (2010) 270–280.
[21] Z.-P. Wang, T. Zhang, Characterization of soluble microbial products (SMP) under stressful conditions, Water Res. 44 (2010) 5499–5509.
[22] X.-S. He, B.-D. Xi, Z.-M. Wei, Y.-H. Jiang, Y. Yang, D. An, J.-L. Cao, H.-L. Liu, Fluorescence excitation–emission matrix spectroscopy with regional integration analysis for characterizing composition and transformation of dissolved organic matter in landfill leachates, J. Hazard. Mater. 190 (2011) 293–299.
[23] D.L. Macalady, K. Walton-Day, New light on a dark subject: On the use of fluorescence data to deduce redox states of natural organic matter (NOM), Aqu. Sci. 71 (2009) 135–143.
[24] Y. Yamashita, A. Panton, C. Mahaffey, R. Jaffé, Assessing the spatial and temporal variability of dissolved organic matter in Liverpool Bay using excitation–emission matrix fluorescence and parallel factor analysis, Ocean Dyn. 61 (2011) 569–579.
[25] Y. Yamashita, R. Jaffé, Characterizing the interactions between trace metals and dissolved organic matter using excitation−emission matrix and parallel factor analysis, Environ. Sci. Technol. 42 (2008) 7374–7379.
[26] R. Jaffé, J. Boyer, X. Lu, N. Maie, C. Yang, N. Scully, S. Mock, Source characterization of dissolved organic matter in a subtropical mangrove-dominated estuary by fluorescence analysis, Mar. Chem. 84 (2004) 195–210.
[27] T. Ohno, A. Amirbahman, R. Bro, Parallel factor analysis of excitation–emission matrix fluorescence spectra of water soluble soil organic matter as basis for the determination of conditional metal binding parameters, Environ. Sci. Technol. 42 (2007) 186–192.
[28] S.A. Baghoth, S.K. Sharma, G.L. Amy, Tracking natural organic matter (NOM) in a drinking water treatment plant using fluorescence excitation–emission matrices and PARAFAC, Water Res. 45 (2011) 797–809.
[29] P. Herzsprung, W. von Tümpling, N. Hertkorn, M. Harir, O. Büttner, J. Bravidor, K. Friese, P. Schmitt-Kopplin, Variations of DOM quality in inflows of a drinking water reservoir: Linking of van Krevelen diagrams with EEMF spectra by rank correlation, Environ. Sci. Technol. 46 (2012) 5511–5518.
[30] Z. Wu, R.P. Rodgers, A.G. Marshall, Two-and three-dimensional Van Krevelen diagrams: A graphical analysis complementary to the Kendrick mass plot for sorting elemental compositions of complex organic mixtures based on ultrahigh-resolution broadband Fourier transform ion cyclotron resonance mass measurements, Anal. Chem. 76 (2004) 2511–2516.
[31] S. Kim, R.W. Kramer, P.G. Hatcher, Graphical method for analysis of ultrahigh-resolution broadband mass spectra of natural organic matter, the Van Krevelen diagram, Anal. Chem. 75 (2003) 5336–5344.
[32] L. Sun, E. Perdue, J. Meyer, J. Weis, Use of elemental composition to predict bioavailability of dissolved organic matter in a Georgia river, Limnol. Oceanogr. 42 (1997) 714–721.
[33] A. Zsolnay, E. Baigar, M. Jimenez, B. Steinweg, F. Saccomandi, Differentiating with fluorescence spectroscopy the sources of dissolved organic matter in soils subjected to drying, Chemosphere 38 (1999) 45–50.
[34] K. Kalbitz, J. Schmerwitz, D. Schwesig, E. Matzner, Biodegradation of soil-derived dissolved organic matter as related to its properties, Geoderma 113 (2003) 273–291.
[35] A. Huguet, L. Vacher, S. Relexans, S. Saubusse, J.M. Froidefond, E. Parlanti, Properties of fluorescent dissolved organic matter in the Gironde Estuary, Org. Geochem. 40 (2009) 706–719.
[36] N. Senesi, Molecular and quantitative aspects of the chemistry of fulvic acid and its interactions with metal ions and organic chemicals, Anal. Chim. Acta 232 (1990) 77–106.
[37] J.J. Mobed, S.L. Hemmingsen, J.L. Autry, L.B. McGown, Fluorescence characterization of IHSS humic substances: Total luminescence spectra with absorbance correction, Environ. Sci. Technol. 30 (1996) 3061–3065.

[38] I.H.S.S. Website 2015. Available from: <http://www.humicsubstances.org>.
[39] H. Books, Articles on Amino Sugars, Including: Streptomycin, Neomycin, Gentamicin, Aminoglycoside, Paromomycin Sulfate, Kanamycin, Tobramycin, Amikacin, Capreomycin, Apramycin, Netilmicin, Hygromycin B, G418, Verdamicin, Sisomicin, Isepamicin, 2011.
[40] T. Bond, O. Henriet, E.H. Goslan, S.A. Parsons, B. Jefferson, Disinfection byproduct formation and fractionation behavior of natural organic matter surrogates, Environ. Sci. Technol. 43 (2009) 5982–5989.
[41] IonSource. Available from: <http://www.ionsource.com/Card/protein/BovineSerumAlbumin.htm>.